

Cite this: DOI: 10.1039/c0xx00000x

www.rsc.org/xxxxxx

ARTICLE TYPE

Structure and Dynamics Studies of the Short Strong Hydrogen Bond in the 3,5-Dinitrobenzoic Acid - Nicotinic Acid Molecular Complex

Samantha J. Ford,^{a,b} Garry J. McIntyre,^{a,c} Mark R. Johnson^b and Ivana Radosavljević Evans^{*a}

Received (in XXX, XXX) Xth XXXXXXXXXX 20XX, Accepted Xth XXXXXXXXXX 20XX

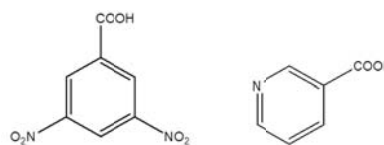
DOI: 10.1039/b000000x

The molecular complex between 3,5-dinitrobenzoic acid and nicotinic acid (35DBNA) has been studied by variable temperature single crystal X-ray and neutron diffraction (30 to 300 K) and *ab-initio* molecular dynamics, in order to investigate the dynamics and any proton migration in this system, which exhibits structural similarities with the well-known proton migration material 3,5-dicarboxylic acid. The refined structures clearly indicate a significant degree of proton transfer in the short NHO hydrogen bond, contrary to the previous description of 35DBNA as an organic adduct without proton transfer. This behaviour is consistent with the difference between the pKa values of 3,5-dinitrobenzoic acid and the ring nitrogen atom in nicotinic acid. Complementary *ab-initio* MD simulations at 400 K show the key proton hopping across the NHO short hydrogen bond, spending short periods along the trajectory (8% of the simulation time) bonded to the O atom. Similar simulations performed on 3,5-dicarboxylic acid and 3,4-dicarboxylic acid show that MD calculations correlate well with experimental observations (or absence) of proton migration, and therefore suggest that they could be used as a predictive tool for investigating this phenomenon in short strong hydrogen bonds.

Introduction

The hydrogen bond is one of the most important chemical interactions in nature and, as such, has important structural and functional roles in a diverse range of systems. Although hydrogen bonds are largely electrostatic in nature, of great current interest are short strong hydrogen bonds (SSHBs) which possess a strongly covalent character. The presence of SSHBs can lead to interesting phenomena, such as temperature dependent proton migration, previously observed by single crystal neutron diffraction in a number of compounds including urea phosphoric acid (UPA)^{1, 2}, 4-methylpyridine pentachlorophenol (MP-PCP)³, 1,2,3,4-tetracarboxylic acid 4,4'-bipyridyl co-crystals (BTA-BPY)⁴, 3,5-pyridine dicarboxylic acid (35PDCA)^{5, 6, 7}, pyridinium 2,4-nitrobenzoate (24PDNB)⁸, 3,5-dinitrobenzoic acid-3,5-dimethylpyridine (35DBA-35DMP)⁹ and dimethylurea-oxalic acid complexes¹⁰.

Interesting proton dynamics in SSHBs and a pronounced isotope effect are found in the four isotopologues of 35PDCA.⁷ 35PDCA forms infinite two-dimensional sheets perpendicular to the *c*-axis, stabilised by a intermolecular hydrogen bonds; a "normal" O...H-O bond of 2.57 Å at 15 K, and a very short strong O...H-N bond of 2.52 Å at 15 K. The proton in the SSHB migrates approximately 0.1 Å from an asymmetric position closer to the pyridyl nitrogen at 15 K to an asymmetric position closer to the carboxylic oxygen at 296 K. In our recent comprehensive study of the isotopologues of 35PDCA, we have found that a first-order isosymmetric phase transition accompanies the deuteron migration of 0.32 Å in *d*-35PDCA;⁷ the magnitude of this effect is the largest observed to-date in this class of compounds.

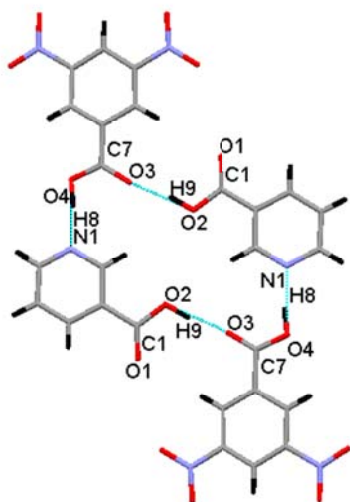


Scheme 1: 3,5-dinitrobenzoic acid-nicotinic acid (35DBNA)

A search of the Cambridge Structural database (CSD)¹¹, carried out to identify compounds with similar structural and hydrogen bonding features, gave a number of potential candidates for further study, including the 3,5-dinitrobenzoic acid - nicotinic acid system (35DBNA, Scheme 1). The structure of 35DBNA was first reported by Zhu and Zheng using X-ray diffraction analysis at room temperature only.¹² This material was found to crystallise in monoclinic space group *P*2₁/*n*, and it is stabilised by a network of hydrogen bonds: a short O4-H8...N1 bond of 2.54 Å, and a normal O2-H9...O3 bond of 2.56 Å (Figure 1). The refined positions of the hydrogen atoms involved in hydrogen bonding suggested no evidence for proton transfer, and the material was described as an organic adduct.¹²

The crystal structure of 35DBNA hence exhibits certain similarities with 35PDCA: it contains two competing intermolecular interactions, a short N...O and a normal O...O contact; these two hydrogen bonds are in a planar arrangement; at room temperature, the proton in the short hydrogen bond is found bonded to the oxygen atom. These structural similarities suggest that temperature-induced proton migration may potentially occur along the short NHO hydrogen bond in

35DBNA in a way similar to that in 35PDCA, *i.e.* that on decreasing the temperature the proton moves away from the oxygen towards the centre of the hydrogen bond and the N atom.



5 Figure 1: Hydrogen bonding in 35DBNA reported by Zhu and Zheng¹²: a short (2.54 Å) N...O contact and a medium (2.56 Å) O...O contact.

To investigate the proton behaviour in this short hydrogen bond, we have undertaken a combined experimental and computational study. In this paper we report the 30 and 300 K structures of 35DBNA determined from single crystal neutron diffraction, and supporting characterisation of this material by variable temperature single crystal and powder X-ray diffraction. The results of complementary density functional theory molecular dynamics (DFT MD) simulations are also reported and they corroborate the experimental findings.

Experimental details

Sample preparation

Crystals of 35DBNA were obtained from the reaction of 3,5-dinitrobenzoic acid (Aldrich, 99%) and nicotinic acid (Aldrich, 98%) in a 1:1 molar ratio; these reagents were used as obtained with no further purification. Crystals suitable for X-ray analysis were grown from water in a 23 cm³ lab scale Parr® General Purpose Acid Digestion Bomb; colourless, rod shaped crystals appeared after 2 hours at 448 K and a slow cooling regime. Larger crystals for neutron analysis were grown by slow evaporation from a 1:2 ethanol:water mixture; colourless, rod shaped crystals resulted after three weeks.

Single Crystal X-ray Diffraction

A crystal measuring 0.08 × 0.20 × 0.24 mm³ was selected for X-ray analysis. Data were collected at four temperatures from 100 to 300 K on a Bruker SMART 1000 diffractometer with a CCD area detector, using graphite monochromated MoK_α radiation. A full sphere of data was collected at each temperature by a series of ω scans, using a frame width of 0.3° in ω and an exposure time of 20 seconds per step. The raw data were collected using the SMART software and integrated using the SAINT suite of

programmes¹³; this included performing an empirical absorption correction in SADABS and reduction in XPREP¹⁴. Structure refinement on F^2 was carried out using CRYSTALS¹⁵. All non-hydrogen atoms were refined anisotropically. Hydrogen atoms were located using difference Fourier maps and refined isotropically; a three parameter Chebyshev weighting scheme was used.

Single Crystal Neutron Diffraction

A crystal measuring 1.1 × 0.8 × 0.5 mm³ was selected for neutron analysis. Single crystal neutron diffraction data were collected on VIVALDI (Very Intense Vertical Axis Laue Diffractometer) at the ILL.¹⁶ This diffractometer uses a white thermal neutron beam and is equipped with a cylindrical image plate detector on a vertical axis. Data were collected at 30 and 300 K; ten diffraction patterns, each accumulated over six hours, were collected at each temperature with successive patterns distinguished by a rotation of 20° of the crystal perpendicular to the incident beam. The Laue patterns were indexed using LAUEGEN¹⁷ and the individual spots integrated using INTEGRATE+ which is a two-dimensional adaption of the three-dimensional min(σ(I)/I) routine.¹⁸ The integrated reflections were normalised to a common wavelength, using a curve derived by comparing equivalent reflections and multiple observations, and corrected for the different angles of incidence, via the program LAUE4.¹⁹ Structure refinement on F^2 was carried out using SHELXTL. Atomic coordinates and anisotropic displacement parameters were refined for all atoms.

Powder Diffraction

Data were collected on a Bruker D8 ADVANCE diffractometer (CuK_{α1,2}), equipped with an Oxford Cryosystems PheniX closed circuit refrigerator. The sample was cooled from 295 to 12 K at a rate of 15 K/hour and, simultaneously, a series of 20 minute patterns were recorded from 5 to 60° using a step size of 0.014°. Temperature was logged throughout the experiment and an in-house routine was used to extract the mean temperature for each range of data. Data analysis was carried out using Topas-Academic.²⁰

Numerical Details

The dynamics of 35DBNA were investigated using the VASP DFT code which uses a plane wave basis set to calculate electronic properties of solids from first principles²¹. PAW pseudopotentials in combination with the PBE functional were used; this gave an energy cutoff of 700 eV. Geometry optimisation was used to determine the initial structure for *ab-initio* molecular dynamics simulations. The simulations presented here were obtained in the NVT ensemble, with a range of temperatures between 30 and 400 K being employed. A time step of 1 fs and a total simulation time of 10 ps were used in each case. The k -point spacing was typically 0.1 Å⁻¹.

Results and discussion

Single crystal X-ray diffraction data collected at four temperatures from 100 to 300 K were analysed and the relevant hydrogen bonding parameters are shown in Figure 2.

Firstly, contrary to the adduct/co-crystal model for 35DBNA proposed by Zhu and Zheng¹², our data suggest a degree of

proton transfer in the short NHO hydrogen bond at all temperatures. This is illustrated in Figure 2a, which shows that the N1H8 distance is shorter than the O4H8 distance at all temperatures. However, the hydrogen atom parameters determined from X-ray diffraction data should be treated with caution, and additional evidence for proton transfer can be sought from the analysis of the C-O distances in the relevant carboxyl groups (Figure 2b). The carboxyl group on the nicotinic acid molecule is only involved in the moderate O-H...O interaction, and the C-O distances of 1.21 and 1.32 Å correspond to double and single bonds, respectively, on the histogram of the carboxyl C-O bond lengths found in the CSD.⁷ On the other hand, the C-O distances in the 3,5-dinitrobenzoic acid group involved in the short N...O hydrogen bond are $d(\text{C7-O3}) = 1.24$ Å and $d(\text{C7-O4}) = 1.26$ Å, suggesting an intermediate character, consistent with a degree of proton transfer away from the oxygen atom O4 towards the nicotinic acid ring nitrogen atom N1.

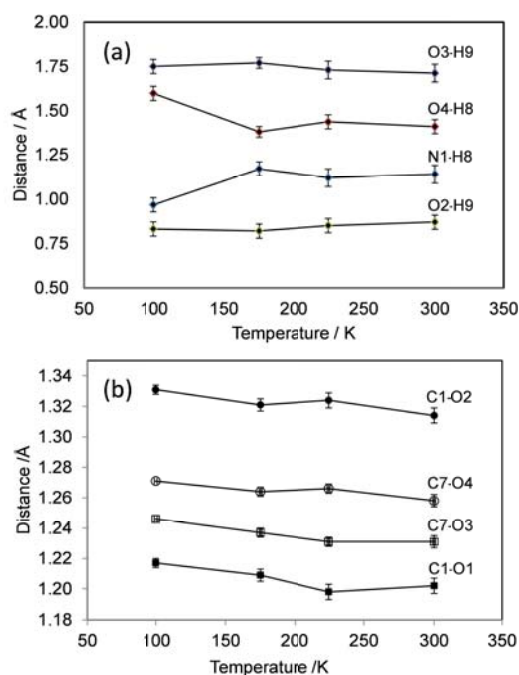


Figure 2: Temperature dependence of the relevant hydrogen bonding parameters obtained from single crystal X-ray diffraction. Lines are drawn as guides to the eye only.

In order to ascertain whether the apparent small discontinuities between 100 and 175 K in the trends shown in Figure 2a represent any real structural changes, we collected variable temperature PXRD data. Subtle structural changes involving hydrogen atoms (such as proton migration or ordering in short hydrogen bonds) can manifest themselves subtly in the unit cell parameter trends obtained from variable temperature powder X-ray diffraction.²² A pure polycrystalline sample of 35DBNA was analysed by powder XRD between room temperature and 12 K to determine the unit cell parameter trends as a function of temperature, and also to obtain accurate unit cell parameters needed for the single crystal neutron Laue diffraction data analysis (*vide infra*).

Data were analysed by Rietveld fitting, in which the fractional

atomic coordinates obtained from single crystal work at room temperature were kept fixed and the parameters refined included unit cell parameters, an overall isotropic temperature factor, sample height displacement, background terms and the peak shape function parameters. The unit cell volume varies smoothly with temperature, showing only the expected thermal expansion (Figure 3). It should be noted, however, that the absence of any clear discontinuities or slope changes in the unit cell parameter trends does not necessarily rule out the possibility of proton migration occurring, as evidenced by the example of 35PDCA.⁷

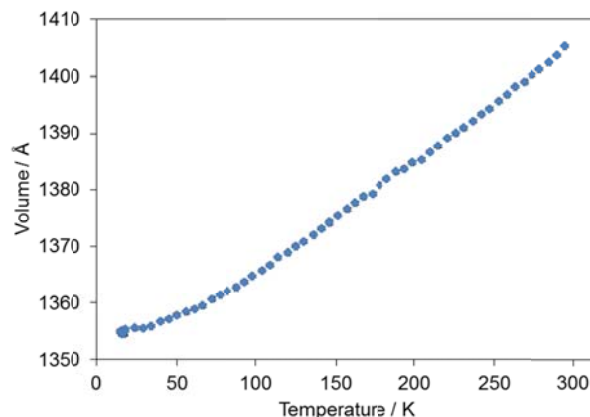


Figure 3: Temperature dependence of the unit cell volume for 35DBNA obtained from powder X-ray diffraction.

Finally, in order to obtain accurate hydrogen atom positions and determine reliably the extent of proton transfer and any temperature-dependent proton migration in the SSHB, the crystal structure of 35DBNA was refined from single crystal neutron diffraction data at 30 and 300 K. The crystallographic details are summarised in Table 1 and the structures are shown in Figure 4; the Crystallographic Information Files have been deposited with CCDC. Since only ratios between unit cell dimensions can be determined in the white-beam Laue technique, it is necessary to use cell dimensions found by some other means; in this case, cell parameters determined from variable temperature powder X-ray diffraction were used. The relevant hydrogen bond parameters determined by single crystal neutron diffraction at 30 and 300 K are summarised in Table 2.

Table 1: Crystallographic details for 35DBNA at 30 and 300 K.

	30 K	300 K
Chemical formula	$\text{C}_{13}\text{H}_9\text{N}_3\text{O}_8$	$\text{C}_{13}\text{H}_9\text{N}_3\text{O}_8$
M_r	335.23	335.23
Space group	$P12_1/n1$	$P12_1/n1$
a (Å)	14.061(6)	14.126(6)
b (Å)	5.039(2)	5.071(2)
c (Å)	19.598(8)	20.163(8)
β (°)	102.641(8)	103.469(8)
V (Å ³)	1354(1)	1405(1)
Z	4	4
D_x (kg m ⁻³)	1.606	1.584
μ (mm ⁻¹)	0.09	0.09
Data collection	Laue method	Laue method
No. measured reflections	13847	10371
No. unique reflections	3018	2171
$R[F^2 > 4\sigma(F^2)]$, $wR(F^2)$, S	0.088, 0.167, 1.09	0.082, 0.157, 0.96
No. observed reflections	3018	2171
No. of parameters	298	298

Table 2: Hydrogen bonding parameters obtained by neutron diffraction.

	30 K	300 K
O4...N1 distance/Å	2.580(5)	2.500(7)
O4...H8 distance/Å	1.436(8)	1.383(15)
H8...N1 distance/Å	1.144(8)	1.119(15)
O2...O3 distance/Å	2.575(4)	2.560(8)
O2...H9 distance/Å	1.010(10)	0.960(17)
H9...O3 distance/Å	1.595(10)	1.617(17)

Full anisotropic structure refinement against the 30 K and 300 K data confirm unequivocally a significant degree of proton transfer in the short hydrogen NHO bond in 35DBNA, from the dinitrobenzoic acid O4 atom to the nicotinic acid N1 atom, as evidenced by the distances listed in Table 2. The ionisation state of molecular complexes can, at least to an approximation, be rationalised by the pK_a values of the relevant acid-base pairs. It is generally expected that a ΔpK_a ($\Delta pK_a = pK_a$ of base - pK_a of acid) greater than 3 will lead to salt formation, while ΔpK_a values below 0 are likely to yield co-crystals; ΔpK_a differences between 0 and 3 correspond to varying degrees of proton transfer (*i.e.* the salt-co-crystal continuum), where other factors such as crystal packing have a significant effect on the ionisation state.²³ Exceptions to the structures expected on these grounds, however, illustrate the problems with using the pK_a values determined in solution to rationalise the behaviour in the solid state.¹⁰ In the case of 35DBNA, the pK_a values of 3,5-dinitrobenzoic acid and of the ring nitrogen atom in nicotinic acid are 2.8 and 4.9, respectively^{24,25}, leading to a ΔpK_a value of 2.1, corresponding to the expected partial proton transfer, consistent with our experimental results.

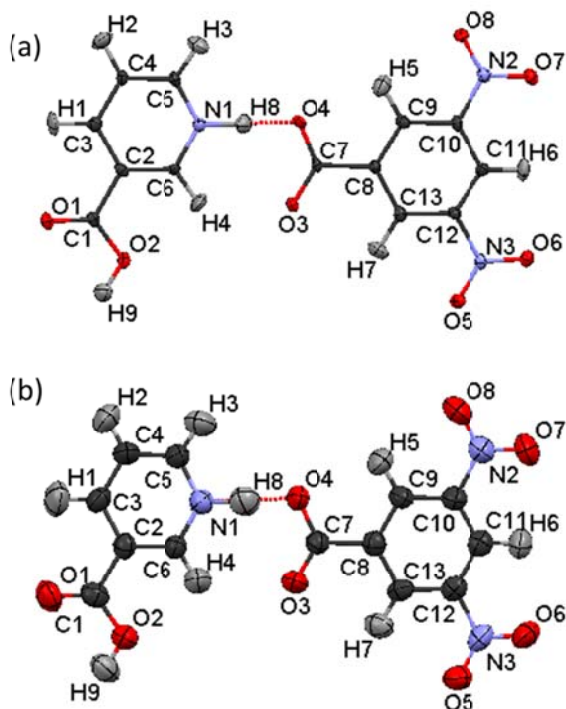


Figure 4: The structure of 35DBNA, as determined by single crystal neutron diffraction at a) 30 K and b) 300 K. ADPs are drawn at the 50 % probability level.

The relatively large standard uncertainties on hydrogen bonding distances listed in Table 2 do not allow us to be conclusive regarding any temperature-dependent proton migration in 35DBNA, given that this is in the majority of cases a subtle effect. One way to quantify the extent of proton migration or transfer is through the hydrogen bond asymmetry, Δ , calculated as the difference between the non-bonded acceptor-hydrogen and the bonded donor-hydrogen distances. For 35DBNA, the hydrogen bond asymmetry parameter is 0.29(1) Å at 30 K and 0.26(2) Å at 300 K. The hydrogen bonding asymmetry values vs. temperature trends in selected well-documented single crystal neutron diffraction-based examples shown in Figure 5. These are predominantly compounds with NHO hydrogen bonds; however, the OHO hydrogen bond of UPA has been shown for completeness. The steeper the line of best fit (Figure 5), the greater the extent of proton migration; migration through the centre of the hydrogen bond is shown by the line of best fit crossing $y = 0$.

We have used computational methods to complement the experimental work, and help shed light on the behaviour of the SSHB proton in 35DBNA. Furthermore, since obtaining large single crystals suitable for neutron diffraction isn't always straightforward, we wished to investigate the predictive power of molecular dynamics (MD) simulations of temperature-dependent behaviour of protons in SSHBs.

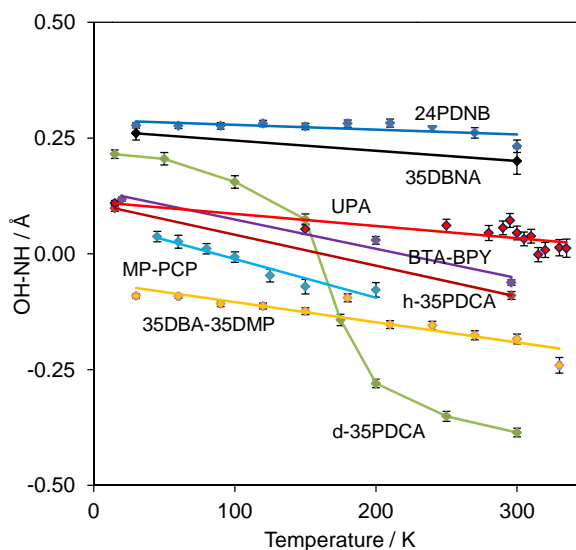


Figure 5: Comparison of the temperature dependence of selected SSHB hydrogen bonding asymmetries, where 24PDBN is pyridinium 2,4-dinitrobenzoate⁸, 35PDCA is 3,5-pyridinedicarboxylic acid⁵, d35PDCA is fully deuterated 3,5-pyridinedicarboxylic acid⁷, BTA-BPY is 1,2,3,4-tetracarboxylic acid 4,4'-bipyridyl¹, MP-PCP is 4-methylpyridine-pentachlorophenol³, 35DBNA is 3,5-dinitrobenzoic acid-nicotinic acid (this paper), 35DBA-35DMP is 3,5-dinitrobenzoic acid-dimethyl pyridine⁹ and UPA is urea-phosphoric acid¹.

The starting structure for MD simulations of 35DBNA was the geometry-optimised structure, in which the residual forces on the

atoms were close to zero. In this model the H8 atom was located at the donor nitrogen atom (N1), with N1–H8 and O4···H8 distance of 1.134 and 1.409 Å respectively; the donor-acceptor distance, N1···O4, was 2.542 Å. These distances are slightly shorter than those observed experimentally at 30 K (Table 2).

MD simulations were undertaken, using the geometry-optimised structure as the starting point, at 15, 100, 200, 250, 300 and 400 K. The variations of the N1–H8, O4···H8, O2–H9 and O3···H9 bond lengths over the course of the trajectory were output using a local routine. The bond lengths are plotted as a function of frame number (time/fs) in Figures 6 a-d.

The plots in Figure 6 reveal the presence or absence of proton hopping in hydrogen bonds. For example, Figure 6b shows proton hopping from one side of the hydrogen bond to the other where the NH and OH bonds (blue and red, respectively) cross. In this case, the length of the OH bond becomes shorter than that of the NH bond, *i.e.* we have an O4–H8 bond and an N1···H8 bond.

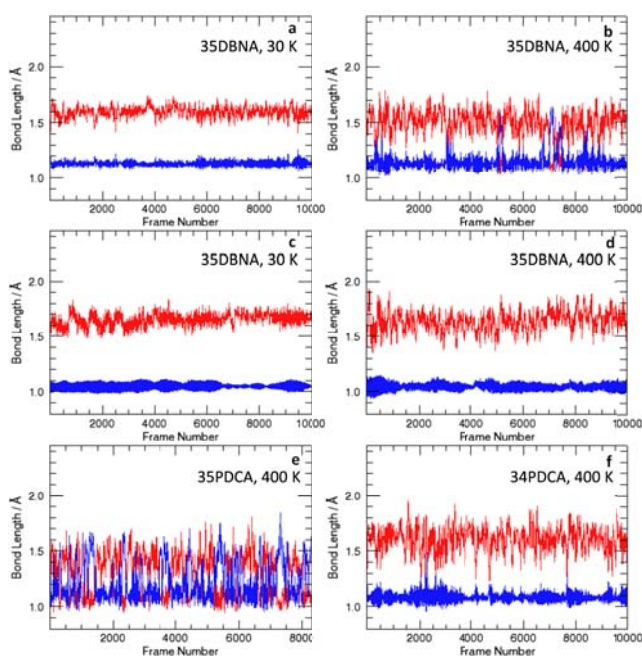


Figure 6: (Top) N1–H8 (blue) and O4···H8 (red) at a) 30 K and at b) 400 K in 35DBNA. (Centre): O2–H9 (blue) and O3···H9 (red) at c) 30 K and d) 400 K in 35DBNA. (Bottom): e) N1–H5 (blue) and O4···H5 (red) at 400 K in 35PDCA and f) O1–H4 (blue) and O3···H4 (red) at 400 K in 34PDCA.

It can be seen that at 30 K no proton hopping occurs (Figure 6a); however, at 400 K, some proton hopping is observed during the course of the simulation (Figure 6b). The possibility that this is simply a thermal effect as a result of the increased temperature is ruled out by the complete lack of proton hopping in the normal O2–H9···O3 hydrogen bond, both at 30 K and at 300 K (Figure 6c and d).

To assess the predictive power of these simulations and their correlation with information obtained from diffraction experiments, a comparison has also been made with two well-established cases: the N1–H5···O4 bond in 35PDCA at 400 K

(Figure 6e) in which a significant proton migration is observed^{5,6,7}, and the O1–H4···O3 bond in 34PDCA at 400 K (Figure 6f) in which no migration is observed experimentally.²⁶ It is clear that the behaviour of the H8 proton in 35DBNA (Figure 6b) is intermediate between these two situations.

The average amount of time that the H8 proton actually spends at the O4 atom in 35DBNA over the course of the MD simulation was calculated as a function of temperature, and the results of this analysis are shown in Figure 7. It can be seen that the value increases smoothly as a function of temperature; however, it seems that the proton cannot be stabilised on the O4 atom for any significant period, spending an average of only 8% of the time in this position at 400 K.

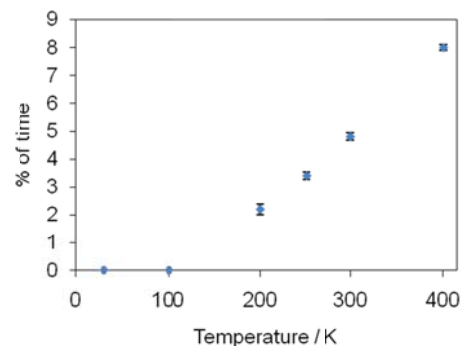


Figure 7: The temperature dependence of the % of time that the H8 proton spends at the O4 atom in 35DBNA.

Conclusions

The molecular complex formed between 3,5-dinitrobenzoic acid and nicotinic acid (35DBNA) has been studied by variable temperature single crystal X-ray and neutron diffraction (30 to 300 K), and *ab-initio* molecular dynamics. The refined structures of 35DBNA in this temperature range clearly indicate significant proton transfer in the short NHO hydrogen bond, contrary to the previous description of this material as an organic adduct without proton transfer. The key hydrogen atom (H8) is located in an asymmetric position closer to the nitrogen atom (N1) rather than the carboxylic acid oxygen (O4), and this partial proton transfer is consistent with the behaviour expected from the difference in the pK_a values of 3,5-dinitrobenzoic acid and of the ring nitrogen atom in nicotinic acid. Relatively large standard uncertainties on the hydrogen bonding distances determined from neutron diffraction at 30 and 300 K preclude clear conclusions about any temperature-induced proton migration. MD simulations at 400 K show the H8 proton hopping across the NHO short hydrogen bond. This proton hopping results in short periods along the trajectory (8% of the simulation time) during which the proton is located at the O4 atom. This is consistent with the structure observed by diffraction at higher temperature being an average structure which into account this proton hopping. Similar simulations performed on 3,5-dicarboxylic acid and 3,4-dicarboxylic acid, known to exhibit and not exhibit temperature-induced proton migration, respectively, show that MD calculations correlate well with diffraction-based observations, and therefore suggest that they could be used as a predictive tool for investigating proton migration in short strong hydrogen bonds.

Acknowledgements

We thank the ILL for beam-time allocation. SJF thanks the ILL and Durham University for a PhD studentship.

Notes and references

^a Department of Chemistry, Durham University, Science Site, South Road, Durham DH1 3LE, UK. Fax: 44 191 3844737; Tel: 44 191 3342594; E-mail: ivana.radosavljevic@durham.ac.uk

^b Institute Laue Langevin, 6 Rue Horowitz, Grenoble Cedex 38, France.

^c Present address: The Bragg Institute, ANSTO, New Illawarra Road, Kirrawee NSW 2232, Australia.

† Electronic Supplementary Information (ESI) available: CIF files

1. C. C. Wilson, *Acta Crystallographica Section B-Structural Science*, 2001, **57**, 435-439.
2. C. C. Wilson and C. A. Morrison, *Chemical Physics Letters*, 2002, **362**, 85-89.
3. T. Steiner, I. Majerz and C. C. Wilson, *Angewandte Chemie-International Edition*, 2001, **40**, 2651-2654.
4. J. A. Cowan, J. A. K. Howard, S. A. Mason, G. J. McIntyre, S. M. F. Lo, T. Mak, S. S. Y. Chui, J. W. Cai, J. A. Cha and I. D. Williams, *Acta Crystallographica Section C-Crystal Structure Communications*, 2006, **62**, O157-O161.
5. J. A. Cowan, J. A. K. Howard, G. J. McIntyre, S. M. F. Lo and I. D. Williams, *Acta Crystallographica Section B-Structural Science*, 2005, **61**, 724-730.
6. F. Fontaine-Vive, M. R. Johnson, G. J. Kearley, J. A. Cowan, J. A. K. Howard and S. F. Parker, *Journal of Chemical Physics*, 2006, **124**.
7. S. J. Ford, Delamore, O. J., Evans, J. S. O., McIntyre, G. J., Johnson, M. R., Evans, I. R., *Chemistry - A European Journal*, 2011, **17**.
8. I. Majerz and M. J. Gutmann, *Journal of Physical Chemistry A*, 2008, **112**, 9801-9806.
9. I. Majerz and M. J. Gutmann, *Rsc Advances*, 2011, **1**, 219-228.
10. A. O. F. Jones, M. H. Lemee-Cailleau, D. M. S. Martins, G. J. McIntyre, I. D. H. Oswald, C. R. Pulham, C. K. Spanswick, L. H. Thomas and C. C. Wilson, *Physical Chemistry Chemical Physics*, 2012, **14**, 13273-13283.
11. F. H. Allen, *Acta Crystallographica Section B-Structural Science*, 2002, **58**, 380-388.
12. J. Zhu and J. M. Zheng, *Chinese Journal of Structural Chemistry*, 2004, **23**, 417-420.
13. Bruker, Madison, Wisconsin, 6.22 edn.
14. G. M. Sheldrick, University of Goettingen, 1998.
15. P. W. Betteridge, J. R. Carruthers, R. I. Cooper, K. Prout and D. J. Watkin, *Journal of Applied Crystallography*, 2003, **36**, 1487.
16. G. J. McIntyre, M. H. Lemee-Cailleau and C. Wilkinson, *Physica B-Condensed Matter*, 2006, **385-86**, 1055-1058.
17. J. W. Campbell, Q. Hao, M. M. Harding, N. D. Nguti and C. Wilkinson, *Journal of Applied Crystallography*, 1998, **31**, 496-502.
18. C. Wilkinson, H. W. Khamis, R. F. D. Stansfield and G. J. McIntyre, *Journal of Applied Crystallography*, 1988, **21**, 471-478.
19. R. Piltz, *Acta Crystallographica* 2011, **A65**, C155.
20. A. A. Coelho, J. S. O. Evans, I. R. Evans, A. Kern and S. Parsons, *Powder Diffraction*, 2011, **26**, S22.
21. G. Kresse and J. Furthmuller, *Physical Review B*, 1996, **54**, 11169-11186.
22. I. R. Evans, Howard, J. A. K., Evans, J. S. O., *Crystal Growth & Design*, 2008, **8**, 1635.
23. S. L. Childs, G. P. Stahly and A. Park, *Molecular Pharmaceutics*, 2007, **4**, 323-338.
24. G. Smith, U. D. Wermuth, D. J. Young and J. M. White, *Acta Crystallographica Section C-Crystal Structure Communications*, 2009, **65**, O543-O548.
25. C. A. Appleby, Wittenbe.Ba and Wittenbe.Jb, *Proceedings of the National Academy of Sciences of the United States of America*, 1973, **70**, 564-568.
26. I. R. Evans, Howard, J. A. K., Evans, J. S. O., Postlethwaite, S. R., Johnson, M. R., *Cryst. Eng. Comm.*, 2008, **10**, 1404-1409.